Journal of Food Measurement and Characterization (2023) 17:167–177
https://doi.org/10.1007/s11694-022-01509-9

ORIGINAL PAPER

Characterization of a novel antimicrobial film based on sage seed gum and *Zataria multiflora Boiss* essential oil

Mansoureh Mohammadi[1] · Reza Yekta[1] · Hedayat Hosseini[1] · Farzaneh Shahraz[1] · Seyede Marzieh Hosseini[1] · Saeedeh Shojaee-Aliabadi[1] · Abdorreza Mohammadi[1]

Received: 16 February 2022 / Accepted: 15 June 2022 / Published online: 13 September 2022

Abstract

As many consumers concern about using synthetic materials to maintain foods' quality and safety, we developed an active packaging based on sage seed gum (SSG) and *Zataria multiflora Boiss* essential oil (ZEO). Pre-test studies indicated that 0.8% SSG (w/v) would be optimum for film preparation based on casting procedure. In the following phase, 1 to 6% ZEO (v/v) was introduced into the film-forming solution. Increasing ZEO concentration significantly lowered tensile strength and elastic modulus without appreciable variation in elongation at break ($P < 0.05$). Antioxidant activity of ZEO-contained films dose-dependently rose from ~ 0% (a film without ZEO) to 38.53% (a film containing 6% ZEO). The active films conferred excellent antimicrobial activity against four biogenic amine-producing bacteria with the highest effect on *Enterobacter aerogenes.* Increasing ZEO concentration resulted in a gradual increment of total color difference (ΔE^*) and opacity. SEM images illustrated improved films' structure homogeneity in terms of ZEO addition up to 3%. According to FTIR curves, ZEO inclusion inhibited formation of hydroxyl bonds between SSG polymeric strands, and resulted in formation of ester bonds between ZEO components and SSG polymer chains. Additionally, it decreased the moisture content and total solubility of the film and improved the water vapor barrier quality. As a result, the usage of SSG films incorporating 2% and 3% ZEO for food packaging applications is advocated.

Keywords Active packaging · Edible film · Sage seed gum · *Zataria multiflora Boiss*

Introduction

Nowadays, the consumers are worried about declining the utilization of synthetic compounds as additives to preserve food products. Moreover, the food industry welcomes using natural products with antimicrobial activity to maintain food quality and freshness during shelf storage without affecting consumers [1, 2].

Edible films, especially those containing natural antimicrobial compounds such as essential oils, are considered excellent packaging for food preservation. The latest films are commonly prepared from biodegradable sources such as proteins, lipids, polysaccharides, or a combination of them [3]. The high permeability of biodegradable films based on polysaccharides and proteins to water vapor, in comparison to synthetic polymer packaging such as plastics, is a major impediment to commercialization [4]. This disadvantage is in terms of the hydrophilic nature of bio-based polymers [3, 4]. However, incorporating lipid compounds such as essential oils, waxes, and fatty acids can minimize the latest issue.

Saliva macrosiphon (sage) flower is an Iranian indigenous plant belonging to the *Saliva* genus. These plant seeds possess a galactomannan-based gum (the ratio of mannose to galactose = 1.78–1.93:1) comprising mostly uronic acids (28.2–32.2%), indicating a polyelectrolyte nature [5]. It has been found that adjusting the solid to water ratio (0.02), pH (6.00), and processing temperature (80.25) increases the gum extraction yield by up to 13.69% [6]. Sage seed gum (SSG) has prospective uses in the food sector owing to its similar properties to commercial hydrocolloids, such as

✉ Saeedeh Shojaee-Aliabadi
s_shojaee@sbmu.ac.ir

✉ Abdorreza Mohammadi
ab.mohammadi@sbmu.ac.ir

[1] Department of Food Science and Technology, Faculty of Nutrition Sciences and Food Technology, National Nutrition and Food Technology Research Institute, Shahid Beheshti University of Medical Sciences, P.O. Box 19395-4741, 1981619573 Tehran, Iran

thickening, emulsifying, and stabilizing actions [7]. Additionally, the research indicated that SSG has favorable film-forming capabilities [5, 7].

Zataria multiflora Boiss, locally known as Avishan-Shirazi, is a medical plant possessing potent aromatic compounds. This plant belongs to the *Labiatae* family and is customarily utilized as a flavoring agent in foods and herbal tea [8]. Its essential oil (ZEO) has high contents of phenolic components, including thymol (~65%) and carvacrol (~4.5%), as well as other compounds such as γ-terpinene (~5.5%) and ρ-cymene (~9%) [9]. The mentioned ingredients have potent antimicrobial and antioxidant properties.

Although there were many studies regarding essential oils as antimicrobial agents in biodegradable films, it is still not scrutinized about their impacts on SSG films' properties and antimicrobial activities against biogenic amine-producing bacteria. Nowadays, biogenic amines have received a great deal of attention due to their adverse health effects, therefore inhibition of their production is of great importance. As essential oils are oily compounds, they can alter biodegradable films' microstructure, barrier and mechanical properties. Therefore, we aimed to investigate the influence of ZEO incorporation into SSG film-forming solution on the physical, mechanical, optical, antimicrobial, antioxidant, and barrier properties of the resulted composite film. To the best of our knowledge, the potential of SSG-based films containing essential oils to apply for food packaging intentions has not been studied yet.

Materials and methods

Materials and bacterial strains

ZEO (≥99.99%) was purchased from Barij Essence Co (Kashan, Iran). SSG (68–76% w/w total carbohydrate) was supplied by Reyhan Gum Parsian Co (Gonbade-Kavoos, Iran). 2,2-diphenyl-1-picrylhydrazyl (DPPH) (≥90%) was provided by Sigma Co (St. Louis, MO). Glycerol (≥99%), Tween 80, calcium chloride ($CaCl_2$) (~90%), sodium chloride (NaCl) (≥99.5%), magnesium nitrate ($Mg(NO_3)_2$) (≥99%), Brain Heart Infusion broth (BHI), Mueller–Hinton Broth (MHB), Mueller–Hinton Agar (MHA), ethanol (≥99.9%) and methanol (≥99.9%) were purchased from Merck Co (Darmstadt, Germany). All other chemicals were of analytical grade.

Morganella morganii PTCC 1078 was supplied by the Iranian Research Organization for Science and Technology (Tehran, Iran). *Enterobacter aerogenes* ATCC 13,048, *Proteus mirabilis* ATCC 7002, and *Klebsiella oxytoca* ATCC 13,182 were provided by Pasteur Institute of Iran (Tehran, Iran). Stock culture of each bacterium was grown in BHI at 37 °C for 24 h before the experiments.

Methods

Film preparation

Preliminary evaluations were conducted to determine the optimal SSG and glycerol (plasticizer) concentrations for film production. It was found that 0.8% w/v SSG produced films with the optimal mechanical characteristics, and the film-forming solutions containing glycerol at a concentration of 60% v/w of SSG peeled off the plates easily.

The film-forming solution was prepared by dissolving 0.8% w/v SSG in distilled water under continuous magnetic stirring at ambient temperature. After complete solubilization of the gum, in order to homogenize the solution and reduce the viscosity, the solution was subjected to ultrasound treatment (Topsonics, Iran) for 10 min (20 kHz, 350 W). Subsequently, the solution was stirred at 800 rpm to eliminate all the air bubbles. Afterward, the glycerol was added to the solution, and stirring was continued for a further 30 min at 25 °C. This approach was employed in the production of control films. To make active films, ZEO was put into stirring solutions after adding Tween 80 (as emulsifier) at a concentration of 10% v/v of ZEO. This resulted in dispersions containing 1 to 6% v/v ZEO. After 30 min of stirring, the solutions were homogenized at 9500 rpm for 1 min at 25 °C using an ultra-turrax (IKA, China). Finally, 100 mL of the solutions were decanted into leveled Teflon plates (153.94 cm^2 surface area) and dried at 30 °C for 18 h. Eventually, the dried films were detached from the casting surfaces and put in the saturated $Mg(NO_3)_2$ solution desiccator (RH = 53%) at 25 °C for 48 h until further evaluation.

Film characterization

Thickness Film thickness was represented as the mean value of at least ten measurements at various points using a micrometer (Mitutoyo, Tokyo, Japan) with a precision of 0.001 mm.

Mechanical properties A texture analyzer (M350-10CT, Testometric Co., Ltd., England) was employed to assess tensile strength (TS), elongation at break (EB), and elastic modulus (EM) of the samples according to ASTM D882-02 [10] at ambient temperature. Five strips (10×1.5 cm^2) from each sample, were equilibrated in $Mg(NO_3)_2$ desiccator (RH = 53%, 25 °C, 48 h) before the test. Preconditioned strips were stabilized between the grips. The initial spacing and cross-head speed were adjusted at 50 mm and 50 mm/min, respectively. Calculations were performed using the following equations:

$$\text{TS (MPa)} = \frac{\text{Maximum force (N)}}{\text{Film cross sectional area (m}^2\text{)}} \quad (1)$$

$$\text{EB (\%)} = \frac{\text{Change in length}}{\text{Initial length}} \times 100 \quad (2)$$

$$\text{EM (MPa)} = \frac{\text{TS}}{\text{EB}} \times 100 \quad (3)$$

Antioxidant properties The films' antioxidant activity was determined using the Brand-Williams et al. [11] technique, which is based on the bleaching of a purple-colored or bluish-red methanol solution of DPPH by an antioxidant [8]. In summary, 25 mg of the film sample was continuously stirred to dissolve it in 5 mL of distilled water. 0.1 mL of this solution was combined with 3.9 mL of methanol solution of DPPH (0.1 mM). The resulting mixture was stored under darkness for 60 min at ambient temperature, and then the absorbance (A) was read at 517 nm against methanol solution of DPPH as blank. DPPH radical scavenging activity (%) was determined according to Eq. 4:

$$\text{DPPH scavenging activity (\%)} = \frac{(A_{\text{blank}}) - (A_{\text{sample}})}{A_{\text{blank}}} \times 100 \quad (4)$$

Antimicrobial properties The antimicrobial activity of the samples was evaluated following an agar disc diffusion method. The film samples were aseptically cut into circular discs (6 mm diameter). They were placed on MHA plates that had previously been inoculated with 100 µL of MHB containing 10^8 CFU/mL of test bacteria. After 48 h incubation at 37 °C, the diameter of inhibition zones (DIZ) was determined by a caliper with an accuracy of 0.02 mm.

Optical properties The color parameters of the film samples, including L^* (lightness), a^* (redness–greenness), b^* (blueness–yellowness), and Op (opacity), were appraised by a HunterLab colorimeter (ColorFlex EZ, Virginia, USA) using a white plate as standard)L_s = 93.98, a_s = -1.33 and b_s = -0.58(based on CIELAB scales. The total color difference (ΔE^*) was determined according to the following equation:

$$\Delta E^* = \sqrt{(L_s - L^*)^2 + (a_s - a^*)^2 + (b_s - b^*)^2} \quad (5) \quad (5)$$

Scanning electron microscopy (SEM) The microstructures of cross-section and surface of film samples were assessed using SEM (VEGA 2, Tescan, Czech Republic). Adhesive tape was used to secure the sample to a copper basis, which was then coated with a platinum coating (SC 7620, England). After cryofractioning the sample in liquid nitrogen, the cross-section area was determined. The images of cross-section and surface were captured using 10 kV accelerating voltage under vacuum pressure (10^{-5} Pa) at the magnification of ×5000.

Fourier transform infrared spectroscopy (FTIR) A Perkin-Elmer FTIR spectrophotometer (Spectrum 1, USA) was used to record FTIR spectra of the film samples at 25 °C using a resolution of 4 cm^{-1} within the range from 450 to 4000 cm^{-1}. Twenty scans were performed for each film sample, and the average was reported.

Thermal properties A thermogravimetric analyzer (TGA 1, Mettler Toledo, Switzerland) was employed for Thermogravimetric Analysis (TGA) of the samples. Analysis was performed in an alumina pan using about 10 mg of the sample under a constant nitrogen flow of 50 cm^3/min at a 10 °C/min heating rate within a temperature range of 25 to 600 °C.

Moisture content (MC) MC was measured by weighing the samples before and after drying at 110 °C to a constant weight. The calculation was performed as follows:

$$\text{MC (\%)} = \frac{(\text{Initial weight}) - (\text{Dry weight})}{\text{Initial weight}} \times 100 \quad (6)$$

Water solubility (WS) WS is defined as the percentage of the film dry matter solubilizes in water after 24 h immersion [12]. The square strip of each sample (2 × 2 cm^2) was weighted (A&D, Japan) to the nearest 0.0001 g after drying at 110 °C to a constant weight (initial dry weight; W_0). The dried sample floated on 50 mL distilled water in a beaker under constant conditions for 24 h at 25 °C. Subsequently, the solution was filtered, and undissolved film particles were dried at 110 °C until a constant weight was reached (dry weight of insoluble material; W_1). WS of each sample was determined by Eq. 7:

$$\text{WS (\%)} = \frac{(W_0) - (W_1)}{W_0} \times 100 \quad (7)$$

Water vapor permeability (WVP) The WVP of the films was measured at 25 °C according to the gravimetric method [13]. The cups (0.00287 m^2 surface area) containing about 100 g anhydrous $CaCl_2$ (RH = 0%) were sealed by the films and put in saturated NaCl solution desiccators (RH = 75%). The water vapor partial pressure was 1753.55 Pa in terms of the difference among RH values of the outer and inner atmospheres of the cups. Weight changes were recorded at 1-h intervals with the precision of 0.0001 g for a period of 10 h. The water vapor transmission rate (WVTR) and WVP were measured using the following equations:

$$\text{WVTR (g/s.m}^2\text{)} = \frac{\text{Slope of weight gain versus time plot(g/s)}}{\text{Exposed film area (m}^2\text{)}} \quad (8)$$

$$\text{WVP (g/m.Pa.s)} = \frac{\text{Film thickness (m)}}{\text{Pressure difference between two sides of the film (Pa)}} \times \text{WVTR} \quad (9)$$

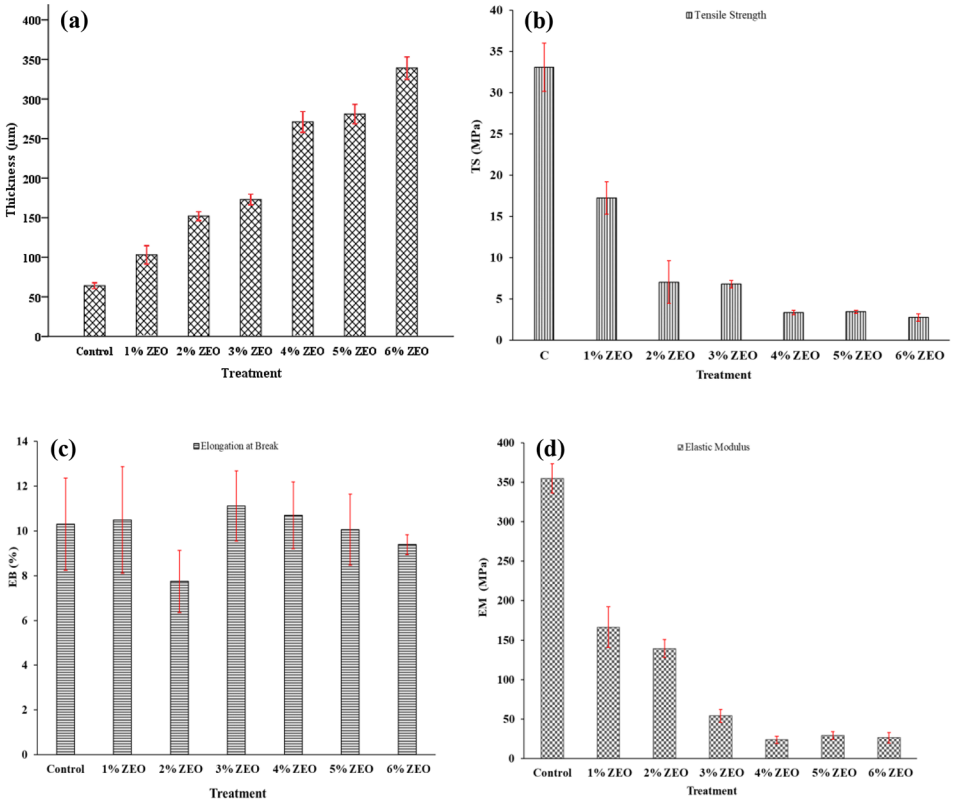

Fig. 1 Thickness (a), tensile strength (b), elongation at break (c), and elastic module (d) of control and ZEO-contained films

Oxygen transmission rate (OTR) The oxygen permeability of the film samples was assessed by a gas permeability tester (GDP-C, Coesfeld, Germany). The films were put in the testing machine cell and sealed. After applying a vacuum in the whole system (5 min), O_2 (99.9% purity) was introduced with the gradient of 0.1 Pa at 25 °C. OTR values were calculated as follows:

$$\mathrm{OTR}(\mathrm{cm}^3/\mathrm{m}^2.\mathrm{d.bar}) = \frac{(\mathrm{Filmthickness}) \times (\mathrm{Mean\ OTR})}{\mathrm{Oxygen\ gradient\ in\ chamber}} \quad (10)$$

Statistical analysis All analyses were performed at least three times, and the means were given. The data analysis was carried out using SPSS statistical software (version 26, SPSS Inc., Chicago, IL). One way analysis of variance followed by Duncan's multiple range tests were used to determine the differences between the samples ($\alpha = 0.05$).

Results and discussion

Mechanical properties

Films' thickness considerably affects optical, barrier, and mechanical properties. Figure 1a shows the alterations in thickness as a result of ZEO incorporation. The control film's thickness was 64 µm, and it significantly increased as the ZEO incorporation dose increased ($P < 0.05$). The latest effect was maximized in SSG film containing 6% ZEO possessing 339 µm thickness. This could be ascribable to ZEO droplets' entrapment among polymeric chains, which subsequently increased the thickness of ZEO-contained films compared with the control [14]. In contrast, Moradi et al. [15] expressed that the zein film's thickness did not significantly change because of the addition of 2% ZEO ($P > 0.05$).

TS, EB, and EM of films are illustrated in Fig. 1b-d. The TS of the control film was 33.11 MPa which was remarkably higher than that reported by Razavi et al. [5] for SSG film (16.56 MPa). This difference might be due to different film preparation procedures as well as gum extraction and purification methods. As observed in Fig. 1, TS significantly declined in terms of ZEO addition (from 33.11 to 2.76 MPa in 6% ZEO film). Besides, about 50% and 75% TS loss was seen to incorporate 1% and 2% ZEO, respectively. This might be explained by the partial replacement of polysaccharide-polysaccharide connections in ZEO-contained films by weaker interactions, e.g., lipid-polysaccharide interactions [14]. As a consequence of these interactions, the cohesion force of the polysaccharide network and the force needed to break the SSG film would decrease. In line with our results, Ghasemlou et al. [16] also stated the exacerbating impact of ZEO and *Mentha pulegium* essential oil (MEO) on the TS of

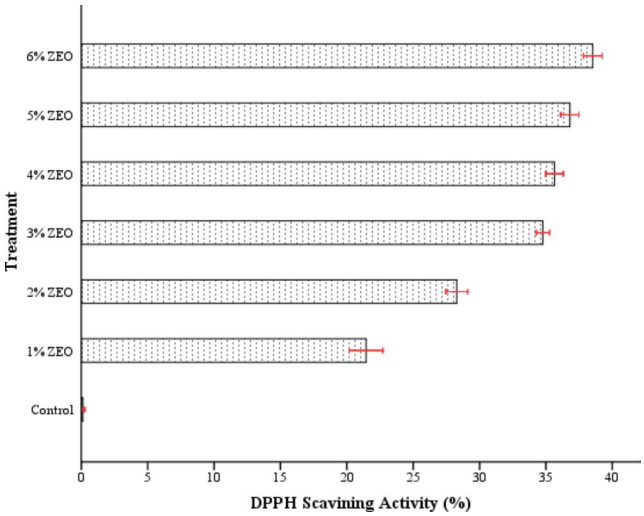

Fig. 2 Antioxidant activity of control and ZEO-contained films

corn starch film. Like the TS pattern, a gradual reduction of EM was seen by increasing the concentration of ZEO. EB is another predominant factor affecting the suitability of coating films for packaging purposes. According to Fig. 1c, the EB of the control film was 10.3% and did not significantly change by the addition of ZEO. This can be explained by the following phenomenon that some lipids cannot create a cohesive and continuous network, leading to decreased or unchanged EB [17].

Antioxidant properties

The films' antioxidant activity was assessed through a DPPH scavenging assay (Fig. 2). The antioxidant activity of the control film was negligible, possibly in terms of the low phenolic compounds of SSG film. As expected, a direct correlation was observed between ZEO content in the films and the related antioxidant activity. In other words, DPPH scavenging activity gradually improved from 21 to 38% by increasing ZEO concentration from 1 to 6%. However, the increment rates were more pronounced in films containing 1, 2, and 3% ZEO. As reported by Dashipour et al. [18] and Sharififar et al. [19], phenolic compounds such as thymol, carvacrol and γ-terpinene are primarily responsible for ZEO's antioxidant activity via quenching free radicals. Although ZEO effectively enhanced the antioxidant activity of SSG films, it showed lower radical quenching activity compared to those stated by Dashipour et al. [18]. Their carboxymethyl cellulose (CMC) film containing 3% ZEO had higher DPPH scavenging activity (82.06%) vs. 3% ZEO SSG film (34.78%). This difference might be due to the different bioactive components profile of the ZEO used in our study. In another study, Moradi et al. [15] observed no significant change in DPPH scavenging activity as a result of increasing ZEO content from 2% (DPPH scavenging activity ~ 27%) to 3% (DPPH scavenging activity ~ 31%) in zein based films due to minimal interactions between protein polymers and ZEO.

Antimicrobial properties

The antibacterial activity of films against four selected spoilage bacterial strains was evaluated by appraising the diameter of inhibition zones (Table 1). As *K. oxytoca*, *E. aerogenes*, *M. morganii*, and *P. mirabilis* are related to biogenic amine production in seafood like tuna fish, the inhibition of their growth is crucial [20, 21]. The native SSG film indicated no inhibitory effect on each of these strains. The film containing 1% ZEO had remarkable antibacterial activity against all four strains, demonstrating the essential oil's potent antimicrobial capabilities against these Gram-negative spoilage bacteria. The antibacterial capabilities were enhanced by raising the ZEO dosage to 3%, and the diameter of inhibition zones did not change substantially ($P > 0.05$) at higher ZEO concentrations. At 3% ZEO, the most sensitive strain was *E. aerogenes* (DIZ: 16.26 mm). In contrast, the most resistant strain was *P. mirabilis* (DIZ: 12.28 mm).

Table 1 The antibacterial activity of control and ZEO-contained films against four selected biogenic amine-producing bacterial strains

Treatments	Diameter of inhibition zones (mm)			
	K. oxytoca	*E. aerogenes*	*M. morganii*	*P. mirabilis*
Control	0^{dA}	0^{eA}	0^{dA}	0^{eA}
1% ZEO	9.53 ± 0.06^{cB}	9.06 ± 0.05^{dD}	10.56 ± 0.07^{cA}	9.17 ± 0.03^{dC}
2% ZEO	11.18 ± 0.03^{bC}	14.18 ± 0.02^{cA}	13.74 ± 0.10^{bB}	10.05 ± 0.04^{cD}
3% ZEO	13.60 ± 0.01^{aC}	16.26 ± 0.03^{bA}	16.14 ± 0.04^{aB}	12.28 ± 0.02^{bD}
4% ZEO	13.61 ± 0.02^{aC}	16.28 ± 0.03^{bA}	16.19 ± 0.04^{aB}	12.29 ± 0.03^{bD}
5% ZEO	13.63 ± 0.01^{aC}	16.30 ± 0.03^{bA}	16.21 ± 0.03^{aB}	12.32 ± 0.01^{abD}
6% ZEO	13.64 ± 0.01^{aC}	16.38 ± 0.03^{aA}	16.23 ± 0.01^{aB}	12.35 ± 0.02^{aD}

All values are mean ± SD

Different small letters in the same column indicate significant differences between the control and ZEO-contained treatments ($p < 0.05$)

Different large letters in the same row indicate significant differences between the microorganisms ($p < 0.05$)

There has not been any information about the antimicrobial properties of films containing ZEO against the latest microorganisms in the literature. Therefore, information about the antibacterial activity of this essential oil against other bacterial species would be investigated. For instance, Dashipour et al. [18] argued the antibacterial effects of CMC films containing ZEO against five pathogenic bacteria, including *Pseudomonas aeruginosa*, *Salmonella typhimurium*, *Escherichia coli*, *Bacillus cereus*, and *Staphylococcus aureus*. They pointed out that ZEO was more effective on Gram-positive bacteria than Gram-negative ones, possibly due to the impermeability of Gram-negative bacteria's outer membrane to lipophilic components. On the other hand, Sharififar et al. [19] found that Gram-negative bacteria were more responsive to ZEO whereas Gram-positive bacteria were more sensitive to a methanol extract of *Zataria multiflora*. The latest disparity may be due to the use of different bacterium strains in those investigations. For example, Sharififar et al. [19] did not investigate the antibacterial activity of ZEO and its extract against *P. aeruginosa*, a Gram-negative bacterium known to be highly resistant to essential oils [22]. To the best of our knowledge, polyphenolic components like carvacrol and thymol are considered predominant ZEO ingredients that hamper microbial growth [19]. These constituents can disrupt the cell membrane by attacking its phospholipid bilayer and damaging enzyme systems [23].

Optical properties

Packaging's color is an important parameter in the viewpoint of customers. Transparent packaging films are usually preferred. The alterations in color parameters (L^*, a^*, b^*, and ΔE^*) resulting from ZEO addition are indicated in Table 2. The lightness of films significantly decreased by adding 1% ZEO. Besides, as ZEO incorporation dose increases, the lightness of films decreases ($P<0.05$). The opposite alteration trends were observed for a^*, b^*, and ΔE^*. These findings were in agreement with visual observations. The latest results could be attributed to the high phenolic content of ZEO, which had light absorption at short wavelengths [18]. Similarly, Shojaee-Aliabadi et al. [14] and Dashipour et al. [18] pointed out that the addition of *Satureja hortensis* essential oil (SEO) and ZEO resulted in diminishing κ-carrageenan and CMC based films' lightness, respectively.

Films' transparency was significantly reduced along with increasing ZEO concentration ($P<0.05$). In other words, by increasing ZEO concentration from 0 to 6%, Op increased from 5.54 to 14.34. This phenomenon might be explained by the light scattering, coalescence, and creaming effects induced by dispensation of EO droplets during the solvent evaporation process of the films [24]. Other publications have found an increase in Op as a consequence of EO integration into bio-based films [14, 18].

Microstructure

Figures 3 and 4 demonstrate the SEM images of the surface and cross-section of the films, respectively. As shown, the control film's surface was completely devoid of cracks and pores. However, the cross-section image revealed several big and tiny holes, suggesting the presence of air bubbles in the control film's structure. It is good to mention that the air bubbles were not recognizable by the unaided eye at the end of the casting process. This may be due to the high viscosity of the SSG film-forming solution in a way that maintained tiny bubbles. Then, during the drying process, the tiny bubbles might aggregate, which created the giant bubbles observed as large halos in the dried film structure [18, 25]. On the contrary, some irregularities appeared on the surface of the films containing ZEO, and they became more pronounced with increasing the essential oil concentration, indicating the heterogeneous structure of the ZEO-contained films. Besides, ZEO incorporation resulted in appearing oval-shaped oil droplets represented in the surface morphology. The spherical shape of oil droplets is usually anticipated in oil in water emulsions. The latest discrepancy could be ascribable to the perpendicular forces actuated by constriction of the SSG network while solvent evaporation [18]. The size of droplets increased with increasing the ZEO concentration. This phenomenon might be attributed to increasing the lipid collision frequency between oil particles in the film matrix [18]. In consequence, the coalescence rate and flocculation of ZEO droplets would rise.

Table 2 Optical properties of control and ZEO-contained films

Film	L^*	a^*	b^*	ΔE^*	Op
Control	82.77 ± 0.33^{a}	-1.06 ± 0.10^{e}	17.68 ± 0.36^{e}	21.43 ± 0.47^{f}	5.54 ± 0.17^{e}
1% ZEO	76.65 ± 1.35^{b}	1.71 ± 0.59^{d}	25.81 ± 1.81^{d}	31.72 ± 2.30^{e}	9.69 ± 0.15^{d}
2% ZEO	72.04 ± 0.94^{c}	5.64 ± 0.47^{c}	34.10 ± 0.64^{c}	41.63 ± 1.10^{d}	10.34 ± 0.18^{c}
3% ZEO	71.85 ± 0.69^{c}	6.83 ± 0.21^{b}	37.91 ± 0.32^{b}	45.14 ± 0.57^{c}	10.74 ± 0.11^{c}
4% ZEO	70.92 ± 0.85^{cd}	7.16 ± 0.12^{b}	38.26 ± 0.46^{b}	45.97 ± 0.34^{bc}	11.94 ± 0.58^{b}
5% ZEO	70.50 ± 0.31^{d}	7.96 ± 0.25^{a}	39.29 ± 1.00^{b}	47.19 ± 1.03^{b}	12.12 ± 0.49^{b}
6% ZEO	70.94 ± 0.82^{cd}	8.21 ± 0.23^{a}	41.09 ± 0.19^{a}	48.56 ± 0.60^{a}	14.34 ± 0.18^{a}

All values are mean ± SD

Different small letters in the same column indicate significant differences between the control and ZEO-contained treatments ($p<0.05$)

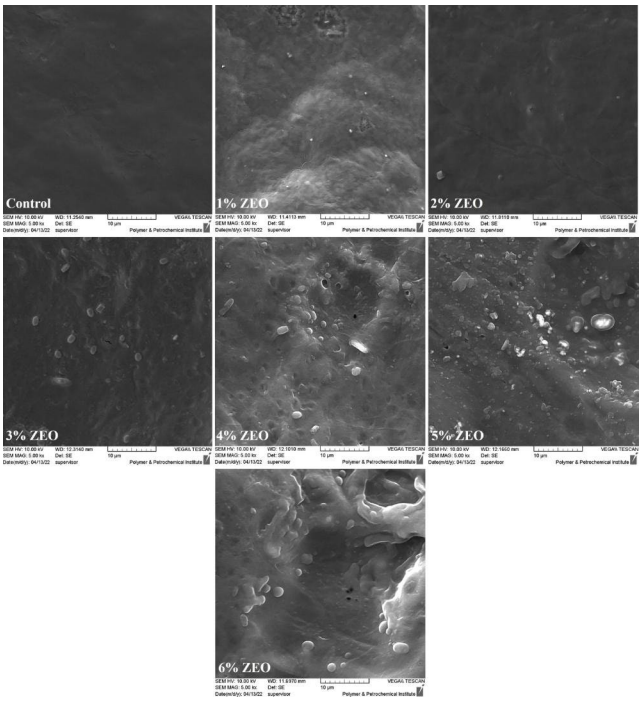

Fig. 3 SEM images of the surface of native and ZEO-contained films presented at a magnification of ×5000

Moreover, the bubbles observed in the cross-section of the control film did not exist in the films containing 1 to 3% ZEO. We hypothesized that ZEO considerably lowered the viscosity of the film-forming solution by interfering with

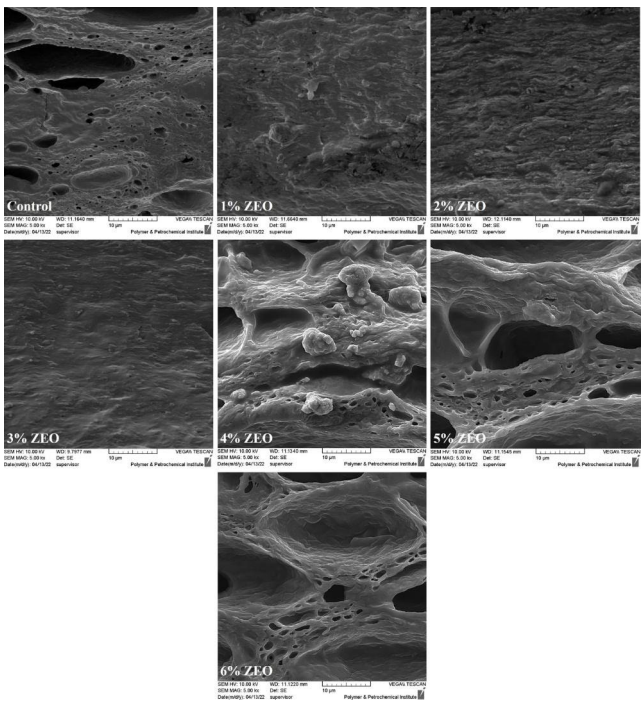

Fig. 4 SEM images of the cross-section of native and ZEO-contained films presented at a magnification of ×5000

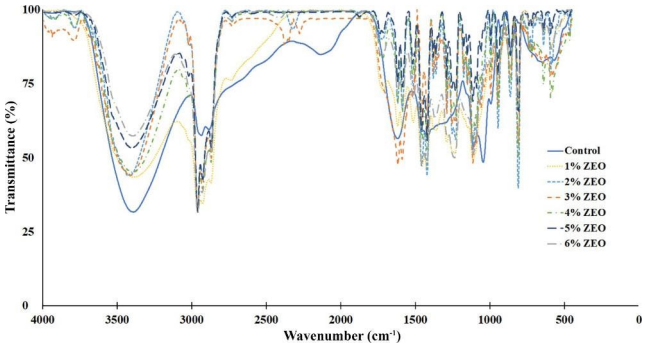

Fig. 5 FTIR curves of control and ZEO-contained films

polymer-polymer interactions between SSG polysaccharide strands, which was validated visually. Therefore, the air bubbles may more readily escape the polymeric matrix of the SSG-ZEO film-forming solution. According to Fig. 4, the porous structure was observed at higher concentrations (> 3%). This could be assignable not only to the ZEO evaporation during drying process, but also to the entrance and entrapment of numerous bubble molecules while applying the ultra-homogenization treatment during sample preparation [25].

FTIR

The FTIR spectra of control film and those containing ZEO were demonstrated in Fig. 5. The broad absorption band in the wavenumber range from 3800 to 3000 cm^{-1} was associated with hydroxyl stretching vibration, arising from hydrogen binding of glucopyranose hydroxyl groups, O—H bonded with carboxylic acid groups (uronic acid), and hydroxyl groups of plasticizer. The peaks between 3000 and 2800 cm^{-1} wavenumbers were due to stretching vibration of –CH in CH_2 and CH_3 groups [26]. Asymmetric and symmetric stretching vibrations of carboxylic acid groups were observed at 1619 and 1425 cm^{-1}, respectively. The absorption peaks between 1184 and 922 were originated from C-O, C-O-C glycosidic, and C-OH bonds. Moreover, the carbohydrate's fingerprint area is located in the wavenumber range of 1200 to 800 cm^{-1}, commonly utilized to compare different structures [27, 28]. Although the anomeric region, 1000 to 800 cm^{-1}, gives us supplemental information, its interpretation is difficult because of overlapping peaks [27].

The intensity of hydroxyl peaks decreased by the ZEO incorporation. Besides, increasing ZEO concentration from 1 to 6% also resulted in the O—H group's peak intensity decrementation. This consequence might be ascribed to the inhibitory effect of ZEO on the formation of hydroxyl cross-links between polymeric chains of SSG. The intensity of peaks at 3000 to 2800 cm^{-1} was increased in films containing ZEO compared with the control film. This could

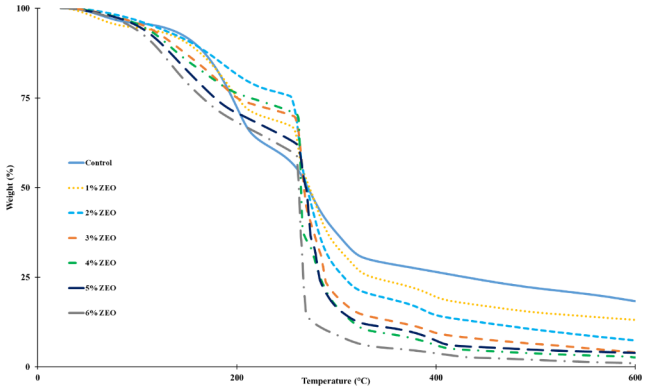

Fig. 6 TGA curves of control and ZEO-contained films

be due to the presence of functional groups containing –CH in ZEO composition. Therefore, the hydrophobic properties of films might be enhanced by decreasing the intensity of hydroxyl groups and increasing –CH groups. The results of these interactions were consistent with those of tensile testing. The more the hydroxyl bonds between polymeric chains, the greater the tensile strength. ZEO decreased the tensile characteristics by decreasing the hydroxyl bonds.

The incorporation of ZEO caused either formation or elimination of several peaks in the FTIR spectra of films. For instance, two adjoining peaks that appeared at wavenumbers 1289 and 1237 cm^{-1} might originate from symmetric and asymmetric stretching vibrations of C-O groups of ZEO's phenolic compounds [27]. In ZEO-contained treatments, two absorption bands appeared at 1586, and 1514 cm^{-1} could correspond to C = C functional groups of aromatic compounds. Furthermore, the formation of new peaks at 812 cm^{-1} in all the treatments containing ZEO indicated bending vibrations of the C-H bonds presented in aromatic components. Thus, the latest evidence suggested the presence of phenolic and aromatic compounds of the essential oil in the film's structure. The peak at 1044 cm^{-1}, which appeared in the control treatment, might be attributed to stretching vibrations of the C-O bond in the C-O-H functional group [29]. On the contrary, ZEO-contained treatments had peaks at about 1716 cm^{-1}, but not the control treatment. This peak might arise from stretching vibrations of the C = O bond related to carbonyl groups of esters. Presumably, the active ingredients of ZEO interacted with C-O-H functional groups of SSG polymeric chains and finally adjoined through ester bonds.

Thermogravimetric analysis

The TGA curves of control and ZEO-contained films are shown in Fig. 6. In the control treatment, three distinct weight reduction zones were found. Water was evaporated in the first region at temperatures ranging from 45 to 120 °C. In the second zone, low molecular weight polymers were destroyed, and glycerol was also evaporated between 120 and 225 °C. The last region was associated with the degradation of the main polymer backbone at 225 to 600 °C [26]. In the films containing ZEO, there was no recognizable border between region I and region II. This could be in terms of the difference among the volatilization temperatures of ZEO components in the way that the two regions were merged. As ZEO components interact with the functional groups of SSG polymer chains, their thermal stability could be enhanced up to a certain dose. For instance, 50% weight loss of control and 1% ZEO films occurred at 270 and 272 °C, respectively. In accordance with the latest result, Zhou et al. [30] observed that the incorporation of 1.5% cinnamon essential oil led to an enhancement in thermal resistance of cassava starch-based films. They explained that the essential oil addition contributed to the formation of new interaction and the improved compatibility among the film's components. However, further increment of ZEO concentration resulted in decrementation in the film's thermal resistance.

The so-called char at 600 °C of control film (17.91%) was considerably higher than ZEO-contained competitors. More to the point, increasing ZEO concentration from 1 to 6% led to decreasing the char from 13.07 to 1.03%. This might be because essential oil was used in the composition of the ZEO-contained films, and its more volatile nature compared to the main film-forming polysaccharide. Moreover, the concentration of free ZEO components increased with the addition of ZEO at higher doses. As a consequence, at higher temperatures (> 300 °C), these volatile compounds evaporate, resulting in a greater weight loss in the 6% ZEO treatment than in the 1% ZEO treatment.

Table 3 Physical and barrier properties of control and ZEO-contained films

All values are mean ± SD

Different small letters in the same column indicate significant differences between the control and ZEO-contained treatments ($p < 0.05$)

Film	WVP (g/m.Pa.s×10^{-10})	OTR (cm^3/m^2.d.bar)	MC (%)	WS (%)
Control	2.88 ± 0.17^{a}	6.62 ± 0.33^{d}	23.23 ± 0.09^{a}	79.00 ± 0.66^{a}
1% ZEO	2.28 ± 0.13^{b}	3.91 ± 0.38^{e}	21.51 ± 0.20^{b}	68.85 ± 1.39^{b}
2% ZEO	1.87 ± 0.14^{b}	2.62 ± 0.25^{f}	19.75 ± 0.22^{c}	61.33 ± 0.45^{c}
3% ZEO	1.41 ± 0.27^{c}	4.09 ± 0.46^{e}	14.99 ± 0.26^{d}	54.93 ± 0.34^{d}
4% ZEO	1.25 ± 0.17^{cd}	7.82 ± 0.16^{c}	13.74 ± 0.09^{e}	49.92 ± 0.35^{e}
5% ZEO	1.11 ± 0.12^{cd}	8.22 ± 0.13^{b}	11.30 ± 0.12^{f}	44.68 ± 0.35^{f}
6% ZEO	0.95 ± 0.19^{d}	12.58 ± 0.65^{a}	10.00 ± 0.16^{g}	40.15 ± 0.27^{g}

Moisture content and water solubility

The MC and WS results of native SSG film and films containing 1 to 6% ZEO were presented in Table 3. ZEO incorporation significantly decreased MC from 23.23% in the control film to 10.00% in SSG film containing 6% ZEO ($P<0.05$). FTIR results confirmed this observation. As essential oils are hydrophobic materials, they influenced the film's affinity toward the water, so its capacity to retain water molecules was declined. In agreement, Ghasemlou et al. [16] reported the decrementation of MC due to either ZEO or MEO incorporation into starch-based films.

In general, film solubility in water depends on the concentration and type of its ingredients, especially their hydrophobicity and hydrophilicity. The inclusion of hydrophobic elements is predicted to decrease solubility, whilst the incorporation of hydrophilic materials is expected to promote solubility [31]. As presented in Table 3, native SSG film had high WS (79.00%), which was higher than that of *Althaea rosea* flower gum film (54.52%) [26], carboxymethyl cellulose film (23.54%) [18], and corn starch film (27.88%) [16].

The solubility of films in water was significantly reduced from 79.00 to 40.15% in control and films containing 6% ZEO, respectively ($P<0.05$). This ~ 49% reduction in WS could be attributed to the increment of film's hydrophobicity due to ZEO incorporation and the less porous structure of the latest films compared with the control film. As seen in SEM images, ZEO considerably decreased the structural porosity of the film, making it difficult for water molecules to penetrate the gap between the polymer chains and thereby solubilize the film. Additionally, the formation of ester bonds between ZEO and SSG chains hampered the binding of water molecules to SSG functional groups such as C-O-H. FTIR results confirmed the latter occurrence. In agreement with the latest results, Ojagh et al. [32] observed 41% and 55% reductions in WS of chitosan films containing 1.5% and 2% cinnamon essential oil than pristine chitosan film, respectively. In another study, do Evangelho et al. [33] reported increasing WS as a result of orange essential oil (OEO) addition in various concentrations (300, 500, and 700 ppm) into corn starch-based films. They proposed that the formation of ruptures in the structure of films because of OEO addition might be the principal reason for this phenomenon. The films with high solubility may have specific applications, for instance, in fruits and vegetable coating, where the film layer is expected to be vanished after washing.

Water vapor and oxygen barrier properties

The results of WVP and OTR of native SSG film and films containing ZEO were reported in Table 3. The WVP of the film without ZEO showed a comparable value (2.88×10^{-10} g/m.Pa.s) considering the WVP of some bio-based films, including chitosan (0.6 to 11.70×10^{-10} g/m.Pa.s) [34, 35], HPMC (6.65 to 9.73×10^{-10} g/m.Pa.s) [36], κ-carrageenan (2.38×10^{-10} g/m.Pa.s) [8], *Lepidium perfoliatum* seed gum (1.68 to 2×10^{-10} g/m.Pa.s) [37], and *Althaea rosea* flower gum (3.14×10^{-10} g/m.Pa.s) [26]. By incorporating up to 6% ZEO, WVP decreased by about 67% compared with the control film. This significant decrease may be attributed to an increase in the hydrophobicity of films containing ZEO, reducing the film's propensity for interacting with water molecules and therefore traveling them within the film's structure. The latest findings corroborated those of previous investigations [8, 14, 16, 18].

In general, there are some parameters, which affect the permeability of either water vapor or oxygen molecules through the film layer, including the chemical structure of polymers, polymer preparation and processing procedures, free volume, orientation, tacticity, polarity, cross-linking and grafting, crystallinity, and presence of additives such as nanomaterials, essential oils and plasticizers [26, 38]. On the whole, increasing density, cross-linking, orientation, crystallinity, and molecular weight can decrease polymer permeability [38].

The OTR of films decreased from 6.62 cm^3/m^2.d.bar to 2.62 cm^3/m^2.d.bar by about 60% as a result of incorporating 2% ZEO. The lowered OTR of the films containing 1 to 3% ZEO might be a result of ZEO filling effect in the SSG polymer structure, as confirmed by SEM. The control film's structure was porous and void-filled, allowing oxygen molecules to pass through readily. By incorporating up to 3% ZEO, those free spaces were filled by ZEO and eventually hampered O_2 permeation [16]. However, the OTR of ZEO-contained films considerably increased along with increasing ZEO concentration up to 6%. In line with our results, Ghasemlou et al. [16] observed a gradual increment in oxygen permeability value due to increasing either SEO or ZEO dose in starch-based films. They explained that the essential oil might accumulate on the films' surface due to adding a high amount of essential oil, subsequently declining the films' surface energy. Consequently, this declined surface energy of films and increased hydrophobicity of the surface could accelerate the O_2 gas absorption from the surrounding atmosphere and finally enhance the solubility of diffusion [16, 39].

Conclusions

We developed a new active packaging film based on SSG containing ZEO. The results of mechanical tests suggested that ZEO addition decreased tensile strength and elastic

modulus, whereas elongation at break did not significantly change. Films containing ZEO demonstrated potent antibacterial activity against all four biogenic amine-producing strains, including *K. oxytoca*, *E. aerogenes*, *M. morganii*, and *P. mirabilis*. The antimicrobial effect of the film containing 3% ZEO was the highest and the lowest on *E. aerogenes* and *P. mirabilis*, respectively. The films' antioxidant activity dose-dependently increased with increasing ZEO content. The optical tests showed that the higher the ZEO content in the film, the higher the ΔE^* and the opacity. ZEO inclusion at the concentrations up to 3% increased the homogeneity of films and decreased their porosity and air bubbles when compared to control film. The latest results indicated that incorporating more than 3% ZEO would not considerably improve antioxidant and antimicrobial properties; moreover, it would decrease films' structural homogeneity, mechanical and optical qualities. The FTIR data indicated that ZEO inclusion resulted in the decrease of –OH bonds and the creation of ester bonds. TGA curves demonstrated that the addition of 1% ZEO slightly enhanced the thermal stability of low molecular weight SSG polymers. MC and WS of films decreased with increasing ZEO concentration up to 6%. The WVP of films reduced by increasing ZEO content. More to the point, 1 to 3% ZEO films obtained lower OTR compared with 6% ZEO and control films. Overall, considering all the parameters, the films containing 2% and 3% ZEO can be suggested as potential films for application in the food industry.

Acknowledgements Financial and technical supports of the National Nutrition and Food Technology Research Institute of Iran are acknowledged. The authors also thank the Iran Polymer and Petrochemical Institute and Institute for Color Science & Technology of Iran for their technical assistance.

CRediT authorship contribution statement **MM**: Project administration, Conceptualization, Methodology, Data curation, Software, Formal analysis, Validation, Investigation, Resources, Writing - original draft, Review and editing, Visualization. **RY**: Methodology, Data curation, Software, Formal analysis, Validation, Investigation, Writing - original draft. **HH**: Project administration, Methodology, Investigation. **FS**: Project administration, Methodology, Investigation. **SMH**: Project administration, Investigation. **SSA**: Project administration, Conceptualization, Methodology, Data curation, Validation, Investigation, Resources, Review and editing, Visualization, Supervision, Funding acquisition. **AM**: Project administration, Methodology, Data curation, Validation, Investigation, Resources, Supervision.

Funding This research did not receive any specific grant from funding agencies in the public, commercial, or not-for-profit sectors.

Data Availability The datasets generated during and/or analyzed during the current study are available from the corresponding author upon reasonable request.

Declarations

Conflict of interest The authors declare that they have no conflict of interest.

References

1. L. Atarés, A. Chiralt, Trends Food Sci. Technol. 48, 51 (2016)
2. GdaS. Dannenberg, G.D. Funck, C.E. dos S. Cruxen, J. de L. Marques, W.P. da Silva, ÂM. Fiorentini, LWT - Food Sci. Technol. 81, 314 (2017)
3. G.L. Robertson, *Food Packaging: Principles and Practice*, 3rd edn. (CRC Press, Taylor & Francis Group, Boca Raton, Florida, 2013)
4. T. Bourtoom, Int. Food Res. J. 15, 237 (2008)
5. S.M.A. Razavi, A. Mohammad, Amini, Y. Zahedi, Food Hydrocoll. 43, 290 (2015)
6. A. Bostan, S.M.A. Razavi, R. Farhoosh, Int. J. Food Prop. 13, 1380 (2010)
7. A.M. Amini, S.M.A. Razavi, Int. J. Biol. Macromol. 162, 1494 (2020)
8. S. Shojaee-Aliabadi, H. Hosseini, M.A. Mohammadifar, A. Mohammadi, M. Ghasemlou, S.M. Hosseini, R. Khaksar, Carbohydr. Polym. 101, 582 (2014)
9. M. Moradi, H. Tajik, S.M. Razavi Rohani, A.R. Oromiehie, H. Malekinejad, J. Aliakbarlu, M. Hadian, LWT - Food Sci. Technol. 46, 477 (2012)
10. ASTM D 882-02, Standard Test Method for Tensile Properties of Thin Plastic Sheeting. (ASTM International, 2002). Www.Astm.Org, http://www.ansi.org
11. W. Brand-Williams, M.E. Cuvelier, C. Berset, LWT - Food Sci. Technol. 28, 25 (1995)
12. N. Gontard, C. Duchez, J.-L. Cuq, S. Guilbert, Int. J. Food Sci. Technol. 29, 39 (1994)
13. ASTM E 96/E 96 M – 05, Standard Test Methods for Water Vapor Transmission of Materials. (ASTM International, 1995). Www.Astm.Org, http://www.ansi.org
14. S. Shojaee-Aliabadi, H. Hosseini, M.A. Mohammadifar, A. Mohammadi, M. Ghasemlou, S.M. Ojagh, S.M. Hosseini, R. Khaksar, Int. J. Biol. Macromol. 52, 116 (2013)
15. M. Moradi, H. Tajik, S.M. Razavi, Rohani, A. Mahmoudian, LWT - Food Sci. Technol. 72, 37 (2016)
16. M. Ghasemlou, N. Aliheidari, R. Fahmi, S. Shojaee-Aliabadi, B. Keshavarz, M.J. Cran, R. Khaksar, Carbohydr. Polym. 98, 1117 (2013)
17. T. Bourtoom, M.S. Chinnan, Food Sci. Technol. Int. 15, 149 (2009)
18. A. Dashipour, V. Razavilar, H. Hosseini, S. Shojaee-Aliabadi, J.B. German, K. Ghanati, M. Khakpour, R. Khaksar, Int. J. Biol. Macromol. 72, 606 (2015)
19. F. Sharififar, M.H. Moshafi, S.H. Mansouri, M. Khodashenas, M. Khoshnoodi, Food Control 18, 800 (2007)
20. D. Nei, S. Kawasaki, Y. Inatsu, K. Yamamoto, M. Satomi, Food Control 28, 143 (2012)
21. S. Phuvasate, Y.C. Su, Food Control 21, 286 (2010)
22. J.C. Matasyoh, J.J. Kiplimo, N.M. Karubiu, T.P. Hailstorks, Food Chem. 101, 1183 (2007)
23. F. Lv, H. Liang, Q. Yuan, C. Li, Food Res. Int. 44, 3057 (2011)
24. B. Ghanbarzadeh, H. Almasi, Int. J. Biol. Macromol. 48, 44 (2011)
25. L. Sánchez-González, M. Vargas, C. González-Martínez, A. Chiralt, M. Cháfer, Food Hydrocoll. 23, 2102 (2009)

26. R. Yekta, L. Mirmoghtadaie, H. Hosseini, S. Norouzbeigi, S.M. Hosseini, S. Shojaee-Aliabadi, Int. J. Biol. Macromol. 158, 327 (2020)
27. M. Tabarsa, M. Anvari, H.S. Joyner (Melito), S. Behnam, A. Tabarsa, Food Hydrocoll. 69, 432 (2017)
28. P. Peng, D. She, Carbohydr. Polym. 112, 701 (2014)
29. J. Jung, Z. Deng, J. Simonsen, R.M. Bastías, Y. Zhao, Sci. Hortic. 200, 161 (2016)
30. Y. Zhou, X. Wu, J. Chen, J. He, Int. J. Biol. Macromol. 184, 574 (2021)
31. K. dos S. Caetano, C.T. Hessel, E.C. Tondo, S.H. Flôres, F. Cladera-Olivera, J. Food Saf. 37, 1 (2017)
32. S.M. Ojagh, M. Rezaei, S.H. Razavi, S.M.H. Hosseini, Food Chem. 122, 161 (2010)
33. J.A. do Evangelho, G. da Silva Dannenberg, B. Biduski, S.L.M. el Halal, D.H. Kringel, M.A. Gularte, A.M. Fiorentini, and E. da Rosa Zavareze, Carbohydr. Polym. 222, 114981 (2019)
34. R.Y. Aguirre-Loredo, A.I. Rodríguez-Hernández, N. Chavarría-Hernández, CYTA - J. Food 12, 305 (2014)
35. M. Pereda, G. Amica, N.E. Marcovich, Carbohydr. Polym. 87, 1318 (2012)
36. A. Jiménez, M.J. Fabra, P. Talens, A. Chiralt, Carbohydr. Polym. 82, 585 (2010)
37. S. Seyedi, A. Koocheki, M. Mohebbi, Y. Zahedi, Int. J. Biol. Macromol. 77, 151 (2015)
38. K.S. Miller, J.M. Krochta, Trends Food Sci. Technol. 8, 228 (1997)
39. J.H. Han, G.H. Seo, I.M. Park, G.N. Kim, D.S. Lee, J. Food Sci. 71, 290 (2006)